Ferroelectric/Semiconductor/Tunnel-Junction Stacks for Nondestructive and Low-Power Read-Out Memory

Ibrahim Burc Misirlioglu and Kursat Sendur

***Abstract*— We demonstrate that a tunnel junction connected in series to the ferroelectric (FE) via a semiconductor (SC) layer can be used to 1 probe the polarization state in an FE thin-film capacitor. A thermodynamic analysis is carried out to demonstrate the carrier depletion and accumulation at the SC/tunnel-junction interface as a function of the polarization direction in the FE layer. Our results indicate that the tunnel junction's polarization and electroresistance depend on those of the main FE bit for a carefully chosen doping of the SC. This would allow measurement of the tunnel current to probe the polarization state of the FE bit nondestructively with much lower power consumption than the destructive technique where the displacement current at the switching of polarization is read. The proposed approach considers an FE/SC/tunnel-junction stack with top and bottom electrodes and is analogous to the Giant Magnetoresistance (GMR) stacks where the resistance change is indicative of magnetization orientation of the pinned and soft layers, implying the binary bit in the storage medium.**

***Index Terms*— Ferroelectric thin-film memory, nondestructive readout, semiconductors (SCs), tunnel junction.**

I. INTRODUCTION

PROBING the bit state of classical state-of-the-art capacitor-type ferroelectric (FE) memory with polarization along the normal of the plane of the sandwiched FE layer is usually carried out destructively by measuring displacement current at switching [1], [2]. In this approach, a fixed electric field higher than the coercive field of the FE is applied via the potential drop between the electrodes. If the polarization sign is opposite of this field, switching occurs that yields a displacement current of roughly $A \times (P_{\uparrow} - P_{\downarrow})/\Delta t$, where P is the polarization normal to the electrodes and $\uparrow, \downarrow$ indicate its direction before and after switching, Δt is the duration of the application of the electric field until full switching has occurred, and A is the electrode area. Upon readout of the displacement current, the binary bit state of the memory is altered for the opposite signs of the field and polarization, requiring a field of opposite sign to rewrite the data. The displacement current is almost zero if no switching has occurred for the same sign of the electric field and initial polarization for a previously written state.

The read-out scheme described in the previous paragraph is power consuming due to the need for polarization switching followed by the rewriting operation of the destroyed data. In addition, it is also vulnerable to leakage currents in the FE layer that can overwhelm the displacement currents. Fatigue on the FE layer emanating from switching the polarization for readout is another problem, reducing the number of possible write cycles and, therefore, the operational lifetime of the device. In fact, the destructive read-out process is one of the limiting steps in FE memory development. The utilization of the displacement current for the read-out process also puts limits on memory size because the current is proportional to the capacitor area. If one tries to overcome this limitation by shortening the switch time via a large electric field for a duration shorter than characteristic switching time, no switching will take place, and hence no read-out is possible. Several approaches have been suggested, including tracking of photocurrents induced inside the FE [3], but such approaches eventually suggest probing currents that can be too small to detect with conventional integrated circuits (ICs) at room temperature (RT). Recently, Nguyen *et al.* [4] suggested the use of MoS_2 sheets for transistor-type action, implying the possibility to access the bit state of the FE by tracking the reflecting and transmitting states under illumination due to carrier-type dependence of MoS_2 on the polarization direction of the underlying FE film. Intermediate electrodes have been employed to sense capacitance changes that would be a function of the polarization direction in an FET-type setting similar to a floating gate approach in flash memories. The same study reported good retention times [5]–[7]. Apart from such approaches, FE tunnel junctions (FTJs) have recently attracted significant attention for nonvolatile memory devices with nondestructive readout [8]–[31]. However, switchable polarization stability in these structures to hold binary data for prolonged times can be a serious concern since the strong built-in fields that form between usually asymmetric electrodes are separated by a few nanometers of the FE.

We propose a metal/FE/SC/FTJ/metal stack for use as solid-state memory where the state of polarization in the FE can be read indirectly via the tunneling currents through the FTJ. Note that although schematically somewhat similar,

Manuscript received February 2, 2016; revised April 7, 2016; accepted April 14, 2016. Date of publication May 3, 2016; date of current version May 19, 2016. This work was supported by The Scientific and Technological Research Council of Turkey under Grant 113M792. The review of this paper was arranged by Editor G.-H. Koh. *(Corresponding author: I. Burc Misirlioglu.)*

The authors are with the Faculty of Engineering and Natural Sciences, Sabanci University, Istanbul 34956, Turkey (e-mail: burc@sabanciuniv.edu; sendur@sabanciuniv.edu).

Color versions of one or more of the figures in this paper are available online at http://ieeexplore.ieee.org.

Digital Object Identifier 10.1109/TED.2016.2555884

0018-9383 © 2016 IEEE. Personal use is permitted, but republication/redistribution requires IEEE permission.
See http://www.ieee.org/publications_standards/publications/rights/index.html for more information.

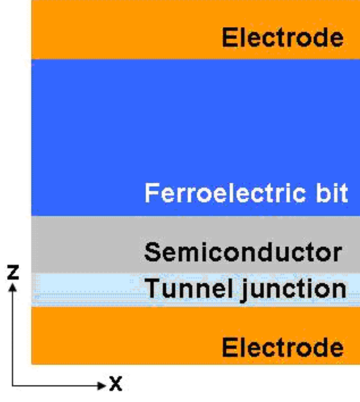

Fig. 1. Schematic of the nondestructive read-out stack studied in this paper.

the way the stack studied in this paper functions rather differently from that of a floating gate in a flash type memory as the latter relies on changes in channel conductivity under a threshold gate bias for a readout of 0 and 1 states. A thermodynamic analysis is carried out to demonstrate the concept where carrier depletion and accumulation at the SC/FTJ interface is a function of the polarization direction in the FE layer. The FTJ is a thin FE that does not exceed 3–4 nm in thickness, allowing a measurable tunneling current when under bias much smaller than the coercive fields. These layers are best suited as electronic valves to control current passage rather than holding binary bits themselves. The stack is close to an electrostatic analog of a Giant Magnetoresistance (GMR) stack functions where high- and low-resistance states indicate antiparallel and parallel states of the magnetization, respectively, in the magnetic layers separated by a thin diamagnetic spacer. Here we show that the current flowing through the FTJ in the stack is expected to be a function of the polarization orientation in the FE bit layer: up and down polarized states in the FE generate electron depletion and accumulation at the FTJ/SC interface that can be probed via tunneling currents during readout.

II. Methodology

As a model system, we take a metal/$BaTiO_3$ (BT)/pSC/BT*/metal stack where * denotes the FTJ layer that is also FE and pSC stands for a p-type SC. The stack can offer reduced power consumption due to the elimination of switching to read the polarization state of the bit. The configuration offers other advantages such as using the FTJ to probe the main bit state, not to retain binary data because of the persisting reliability challenges of such ultrathin layers [21]. The schematic illustration of the stack is given in Fig. 1. A 2-D slice of the structure is considered and the analysis reduces to an x- and an z-axis. We assume the top/bottom electrodes as ideal. The total thickness of the BT/pSC/BT* is 40 nm and we partition the grid (from top to bottom) as 20 nm of the FE, 17 nm of nSC, and 3.2 nm of BT*. The stack for the numerical analysis consists of 100×100 cells along the x- and z-axis. The grid cell size is 0.4 nm, almost the unitcell dimension of BT. The equations of state for the FE layer, the tunnel junction, and the SC are

$$2\alpha_3^m P_z + 2\alpha_{13}^m P_z P_x^2 + 4\alpha_{33}^m P_z^3 + 6\alpha_{111} P_z^5 + \alpha_{112}(2P_z P_x^4 + 4P_z^3 P_x^2) - G\left(\frac{\partial^2 P_z}{\partial z^2} + \frac{\partial^2 P_z}{\partial x^2}\right) = -\frac{\partial \phi}{\partial z} \quad (1)$$

$$2\alpha_1^m P_x + 2\alpha_{11}^m P_x^3 + 2\alpha_{13}^m P_x P_z^2 + 6\alpha_{111} P_x^5 + 2\alpha_{112}[2P_x^3 P_z^2 + P_x P_z^4] - G\left(\frac{\partial^2 P_x}{\partial z^2} + \frac{\partial^2 P_x}{\partial x^2}\right) = -\frac{\partial \phi}{\partial x} \quad (2)$$

in the FE bit layer and the FTJ, where (1) links the out-of-plane component of polarization, P_z to the z-component of electric field, and $E_z = -\partial\phi/\partial z$ with ϕ being the electrostatic potential. Similar to (1), (2) links P_x to E_x, where $E_x = -\partial\phi/\partial z$. α_3^m, α_{13}^m, α_{33}^m, α_1^m, and α_{11}^m are the renormalized phenomenological coefficients in SI units with α_1^m and α_3^m being $\alpha_1^m = \alpha(T - T_C) - u_{ij}^M(Q_{11} + Q_{12})/(S_{11} + S_{12})$ and $\alpha_3^m = \alpha(T - T_C) - 2u_{ij}^M Q_{12}/(S_{11} + S_{12})$, respectively, due to renormalization with misfit strain where $\alpha = (2\varepsilon_0 C)^{-1}$, α_{12}^m and α_{33}^m contain the clamping effect of the film (see [32]), while α_{111} and α_{112} are the dielectric stiffness coefficients in the bulk for BT, and u_{ij}^M is the misfit strain for cubic BT on ST taken as -2.56%, keeping the FE polarization along the normal of the stack. G is the gradient energy coefficient and is assumed to be isotropic for convenience, with a value of 10^{-10} J m^3 C^{-2} [33]. The Maxwell equation is satisfied everywhere inside the stack

$$\nabla \cdot \vec{D} = \rho \quad (3)$$

with $\vec{D}$ denoting the dielectric induction given as

$$\vec{D} = [D_x\hat{x} + D_z\hat{z}] \quad (4)$$

where

$$D_x = \varepsilon_o\varepsilon_b E_x + P_x \text{ and } D_z = \varepsilon_o\varepsilon_b E_z + P_z \quad (5)$$

in the FE and FTJ layers with x and z denoting the in-plane and out-of-plane components, respectively. In the SC

$$D_x = \varepsilon_0\varepsilon_r E_x \text{ and } D_z = \varepsilon_0\varepsilon_r E_z \quad (6)$$

where ε_r is the dielectric constant. In (5) and (6), ε_o is the permittivity of the vacuum and ε_b is the background dielectric constant (see [34 and 35, (7)]) of the FE. Note that (3) contains the derivatives of P_z and P_x that lead to the formation of depolarizing fields at the interfaces where P_z terminates normal to the plane of the stack. The free charge in (3), ρ, has the form $\rho = q(-n^- + p^+ - N_A^-)$ where q is the unit charge and

$$N_A^- = N_A\left(\exp\left(\frac{q(E_A - E_F - \phi)}{kT}\right) + 1\right)^{-1} \quad (7)$$

$$n^- = N_C\left(\exp\left(\frac{q(E_C - E_F - \phi)}{kT}\right) + 1\right)^{-1} \quad (8)$$

$$p^+ = N_V\left[1 - \left(\exp\left(\frac{q(E_V - E_F - \phi)}{kT}\right) + 1\right)^{-1}\right] \quad (9)$$

TABLE I

BAND PARAMETERS, IONIZATION ENERGIES OF ACCEPTORS AND LINEAR DIELECTRIC CONSTANTS OF THE pSC, AND THE FE/FTJ USED IN THE CALCULATIONS. $m^{-3}E^{-1}$ IS THE UNIT FOR DENSITY OF STATES (E: ENERGY UNIT). THE UNITS OF N_C, N_V, AND N_A ARE $cm^{-3}E^{-1}$

	E_F (eV)	N_C	N_V	N_A	E_A (eV)	E_C, E_V (eV)	ε_r (ε_b in FE)
pSC	-5.3	10^{19}	10^{19}	10^{17}	-0.05	-4.05, -5.15	10
FE, FTJ	-4.8	10^{18}	10^{18}	none	none	-3.2, -6.4	7

where N_A^- (N_A) is the ionized (total) acceptor density in the pSC, n^- is the electron density, p^+ is the hole density, N_C is the effective density of states at the bottom of the conduction band, N_V is the effective density of states at the top of the valence band, E_C is the energy of an electron at the bottom of the conduction band, E_V is the energy of an electron at the top of the valence band, E_F is the Fermi level, and E_A is the ionization energy of the acceptor atom that is taken with respect to the top of the valence band. The E_F of the stack is taken as that of the metal electrodes as one expects the electrochemical potential to equilibriate with that of the electrodes. The values of the FE/FTJ, the SC, and the metal work functions are provided in Table I.

Equations (1)–(3) are subject to boundary conditions (BCs) for polarization and electrostatic potential. For the z-axis, these are

$$\phi_{\text{Bottom}} = 0 \text{ when } \phi_{\text{Top}} = V_{\text{Write}} \text{ and } \phi_{\text{Top}} = 0 \text{ when } \phi_{\text{Bottom}} = V_{\text{Read}}, \text{ else } \phi_{\text{Bottom}} = \phi_{\text{Top}} = 0 \quad (10)$$

for electrostatic potential and

$$\lambda \frac{\partial P_x}{\partial x} - P_x = 0|_{z=0(-d),h(-d-t)} \quad \lambda \frac{\partial P_z}{\partial z} - P_z = 0|_{z=0(-d),h(-d-t)} \quad (11)$$

for the polarization BCs where 0 ($-d$) and h ($-d-t$) denote the FE/pSC (FTJ/pSC) and FE/metal (FTJ/metal) interfaces for the bit (FTJ) layer, respectively. λ is the extrapolation length defining how steeply polarization varies before terminating at an interface (taken as much larger than film thickness here, meaning no special surface effects). Periodic BCs are used along the plane of the stack (x-axis). We solve (1)–(3) numerically for the write step (formed by the ± 3 V top electrode bias while the bottom is grounded) that writes a polarization state in both the FE and the FTJ depending on the sign of this field. The application of the ± 3 V bias is sufficient to align P_z in the FE and FTJ and the results provided in the next section is for the 0 V bias step following the write step to check if the written state remains. A write step is evaluated after 10 000 iterations after which we do not see any changes in the stack evolution. Thus, a 0 V/$\pm$3 V/0 V sequence corresponds to 30k iterations and we give the results for 0 V following the write step. The pSC has 10^{23} dopants/m^3 as we find that a moderately doped pSC provides the best interaction between the FE and the FTJ after several trials including n-type SC parameters. The read cycle is considered to be a small voltage pulse on the bottom electrode, far from being an equilibrium process, whose duration is much shorter than the characteristic switching time of an FE but sufficient to allow tunneling (a ns or less). Note that due to the nucleation and growth process, E_{Write} could be less in real systems.

To estimate the tunneling currents during readout that would indicate whether the FE bit is in up or down polarized state, we employ the Wentzel–Kramers–Brillouin (WKB) approximation whereby the potential barrier to carrier tunneling is already obtained from the solution of the thermodynamic equation of state and the Poisson equation whose details are given in the previous paragraphs. The tunneling current can be estimated as

$$J = q v_R n(\text{SC}/\text{FTJ}) T(E) \quad (12)$$

where q is the elementary unit charge, $T(E)$ is the tunneling probability of an electron over an arbitrary barrier, and $V_0(r)$ with an energy E given by (WKB approximation)

$$T(E) = \frac{16E}{V_0}\left(1 - \frac{E}{V_0}\right) e^{\int_0^d -\frac{2}{\hbar}\sqrt{2m(V_0(r)-E)}dx} \quad (13)$$

and v_R is the Richardson velocity found from $v_R = (kT/2\pi m)^{1/2}$, where k is the Boltzmann constant, T is temperature in Kelvin, and m is the electron mass (assumed as rest mass in our calculations), h is the reduced Planck constant, and $n(\text{SC}/\text{FTJ})$ is the electron population density at the pSC/FTJ interface.

Tunneling process timescales, much less than a nanosecond, are much shorter than those needed for switching (see [36] and [37]). With this in mind, as mentioned previously, the read-out pulse would be a small ($\ll$ coercive bias) rapid signal to allow tunneling, but will not perturb the polarization states in both the FTJ and the FE, and is a nonequilibrium phenomenon for the system and no numerical solution of the polarization states under this short pulsed signal is pursued. During the read-out pulse, a fixed voltage of $+0.25$ V appears to be sufficient (applied to the bottom electrode while the top is grounded) to generate tunneling currents on the order of microamperes for accumulation or almost no tunneling when there is carrier depletion at the pSC/FTJ interface depending on the polarization state inside the bit. Considered barrier functions in accordance with our results are provided in the next section. Measurable tunneling currents on the order of a few microamperes in Pb, Zr, TiO_3/La, Sr, MnO_3 [31] and La, Sr, MnO_3/BT/La, Co, MnO_3 [38] ~3-nm-thick FTJ structures without switching were already reported. Read-out voltages in these FTJs did not exceed the 0.1–0.4 V range.

III. RESULTS AND DISCUSSION

Fig. 2 provides the RT P_z results for the write and read cycles mentioned above. After the writing cycle, we find a single domain solution of the FE bit at 0 V bias. Both the FE and FTJ have positive or negative polarization depending on the sign of the write bias [Fig. 2(a) and (b)]. Due to the

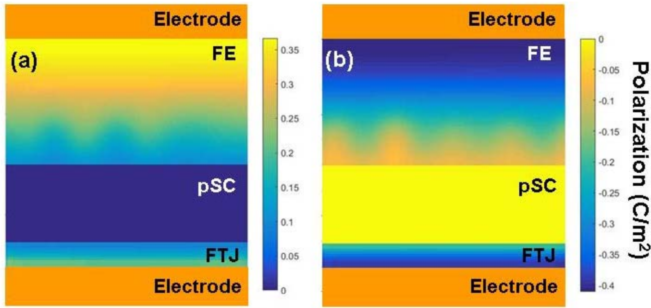

Fig. 2. Polarization maps for (a) +3 V on the top electrode after writing and (b) −3 V on the top electrode after writing. Note that the polarization in the FE and the FTJ is aligned upon writing.

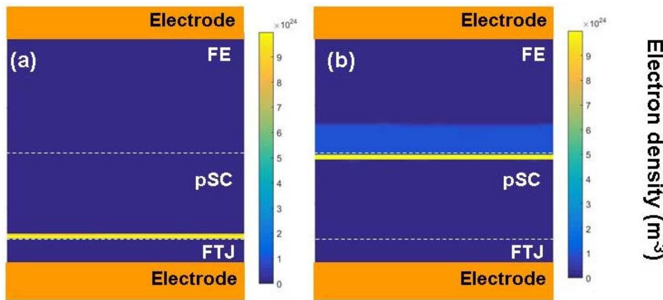

Fig. 3. Conduction electron density maps at 0 V bias for (a) after +3 V writing via the top electrode (up state) and (b) after −3 V writing via the top electrode (down state). Note the electron accumulation at the FE/pSC and FTJ/pSC interfaces for the two different states of polarization in the FE bit layer.

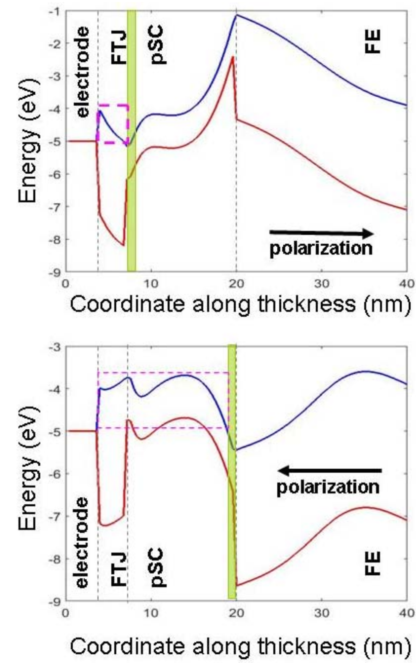

Fig. 4. Flat band energy diagrams for the up state of polarization in the FE bit (top) and the down state of polarization in the FE bit (bottom). The blue line is for the conduction band and the red line is for the valence band. The green shaded strips in both plots indicate the region of electron accumulation for the given state of the FE bit. The arrows indicate the polarization direction in the FE bit layer. The purple dashed square and the purple dashed rectangle in the top and bottom, respectively, emphasize the potential barriers to tunneling. The up state of the FE bit induces a triangular barrier, while the down state barrier is much more complex and larger.

difference in the work functions of the metal and the SC, there will be a built-in bias field in both the FE and the FTJ that could favor the single domain state for a not too thick FE bit layer. This would mean that if the SD state can exist in either polarization state, one will be metastable relative to the other. The built-in bias in many works is accounted for by adding a built-in field term to the total electric field in the FE that consists of the difference in the work functions of the electrodes divided by the film thickness, but such simplifications do not allow an understanding of the position-dependent carrier accumulation/depletion behavior. While we can show in Fig. 2(a) and (b) that an almost SD state is possible after the write cycle, a unique response needs to be attained from each FE bit state during the read bias. The distribution of electrons at 0 V bias following the write step are in Fig. 3(a) and (b), indicating the electron accumulation and depletion at the pSC/FTJ interface for the up and down states of the FE bit, respectively. A tunneling current during the readout whose magnitude differs substantially for both polarization states of the bit layer would serve as a means to probe the bit state. From Fig. 4, it is clear that the electrons near the pSC/FE interface (down state of the FE bit) will see a much thicker barrier, and hence a much lower tunneling current should be expected as we show. Such a difference is expected to lead to tunneling currents during readout that is orders of magnitude different for the two states of the bit layer: almost no current indicates the bit state as up and a measurable tunnel current denotes the bit state as down. A bias value of around 0.2 or 0.25 V for readout appears to be feasible as it has been shown to generate tunneling currents of the order of a few microamperes or more (see [23] and [38]).

It is imperative to discuss the possibility of a single domain–multi domain (SD–MD) state transition: the FE bit layer could undergo an SD–MD transition following the write cycle and we do not find an MD state here after the removal of the write field although P_z can have some position dependence [see Fig. 2(a)]. This does not mean that the SD state is stable: it could be metastable (or perhaps even unstable [33]) under the usual electrical BCs of the bit layer where, in particular, finite screening of the bound charges from the pSC side is considered. The latter is accounted for in this paper as a result of the solution of the Maxwell equation inside both the pSC and the FE/FTJ with the charge density terms coming from the Fermi–Dirac function. The numerical solution process can also fall into a local minimum in the energy landscape although we arrive at the SD state after every cycle. A similar paradox also exists in real applications: thermodynamic results point out the ultimate stability of the MD state whenever the finite screening effects of the electrodes are accounted for [33], [39], but in the meantime, many groups exploit the SD state hysteresis to retain data.

From the point of view of thermodynamic theory, the time-dependent Landau–Ginzburg equation of state could be used, but this would have a meaning only for domain dynamics

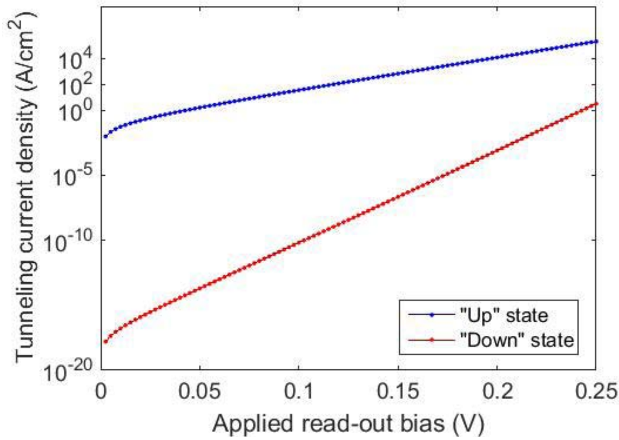

Fig. 5. Tunneling currents computed (a) exactly for the up state of the FE bit and (b) approximately for the down state of the bit.

and switching under a perturbation. The lifetime (or survival period) of the SD state in FE films is a parameter not accessible by thermodynamics, which implies that experiments are needed to assess the survival of the SD state following the write field.

Finally, we give the tunneling current plots we estimated for the two barriers corresponding to the up and down states of the bits consecutively. The barrier in the FTJ forming in the case of the up state of the FE bit is almost a vertical triangle with a maximum potential height of ~0.7 V and the barrier length is the thickness of the FTJ (due to electron accumulation at the SC/FTJ interface). Such a barrier we define as $V_0 x/d$ where x is the coordinate of the pSC/FTJ interface (0 for tunneling calculation) and d is the thickness of the barrier (thickness of the FTJ). In the case of the FE bit in down state, electron accumulation is near the FE/SC interface where the electrons would see a much thicker semicircular-like barrier with some irregular potential variations near the interfaces. Note that the barrier thickness in this case is almost three times the former and are emphasized as the portion of the conduction bands inside the dashed purple lines in Fig. 4.

The integration term in $T(E)$ (13) for the up bit barrier approximated as a triangular shape ($V_0 x/d$, $0 \leq x \leq d$) can be found as $-(2/\hbar)d(\sqrt[3/2]{2\text{m}(V_0/d - E)}/3\ \text{mV}_0)$.

The current density estimated from (12) as a function of electron energy in the limit $E < V_0$ for up and down bit states are in Fig. 5. Clearly, there are about four orders of magnitude in the tunneling current densities corresponding to the two states of the FE bit even at 0.25 V of read-out bias, allowing one to design a memory device around the nondestructive read-out concept put forth in this work. While tunneling phenomena occurs in timescales of attoseconds, momentary depletion of carriers might occur in the SC (that is not a floating layer in contrast to flash and NAND) and that dielectric relaxation times of the pSC might have an influence on the tunneling current's time dependence. Still, the dielectric relaxation times in a doped SC such as a pSC does not exceed a few picoseconds and we expect the read-out step to be much faster than characteristic switching times of the FE and the FTJ, providing the possibility to conduct nondestructive low-power readout keeping in mind the very small bias signs involved here as well.

IV. Conclusion

In summary, using thermodynamic theory coupled with equations of SCs, we demonstrate the concept of a metal/FTJ/SC/FE/metal stack, a solid-state memory device with a nondestructive low-power read-out capability. Using the FTJ as a current valve to tap the binary data of the FE bit is the motivation for this paper for the given reliability challenges associated with FTJs holding binary data. The stack is in analogy with a GMR stack where the resistance (tunnel current in our case) depends on the relative signs of the hard/pinned and soft layers. In principle, because the need to detect the displacement current at switching for readout is eliminated, polarization in leaky FEs could also be read under short bias pulses on the bottom electrode. Moreover, the device size can be smaller than that of conventional FE memories as the requirement of a displacement current being greater than the noise of the ICs during readout at RT is eliminated. We also considered tailoring changes of the electronic character at an FE/metal or an FE/SC interface for nondestructive readout where the interface might become a Schottky type or Ohmic like depending on polarization direction [40], [41]. We did attempt to test this idea as a means of carrying out a nondestructive readout, but our results at the moment are inconclusive. We find that two FE layers, one being the FTJ, interact with one another via an SC medium has well-defined consequences in terms of distinguishing the polarization states as revealed by the tunneling current estimates for the two states of the FE bit. Finally, variants of the stack proposed here can be developed that are even more efficient and integrable into high-density solid-state array architectures.

Acknowledgment

The authors would like to thank J. V. Mantese of United Technologies Research Center for a stimulating discussion.

References

[1] J. F. Scott and C. A. P. de Araujo, "Ferroelectric memories," *Science*, vol. 246, pp. 1400–1405, Dec. 1989.

[2] D. W. Bondurant and F. P. Gnadinger, "Ferroelectrics for nonvolatile RAMs," *IEEE Spectr.*, vol. 26, no. 7, pp. 30–33, Jul. 1989.

[3] L. Pintilie, I. Vrejoiu, G. Le Rhun, and M. Alexe, "Short-circuit photocurrent in epitaxial lead zirconate-titanate thin films," *J. Appl. Phys.*, vol. 101, p. 064109, Mar. 2007.

[4] A. Nguyen *et al.*, "Toward ferroelectric control of monolayer MoS_2," *Nano Lett.*, vol. 15, pp. 3364–3369, May 2015.

[5] Y. Kato, T. Yamada, and Y. Shimada, "0.18-μm nondestructive readout FeRAM using charge compensation technique," *IEEE Trans. Electron Devices*, vol. 52, no. 12, pp. 2616–2621, Dec. 2005.

[6] S. Horita and B. N. Q. Trinh, "Nondestructive readout of ferroelectric-gate field-effect transistor memory with an intermediate electrode by using an improved operation method," *IEEE Trans. Electron Devices*, vol. 55, no. 11, pp. 3200–3207, Nov. 2008.

[7] Y. Kaneko, H. Tanaka, M. Ueda, Y. Kato, and E. Fujii, "A dual-channel ferroelectric-gate field-effect transistor enabling NAND-type memory characteristics," *IEEE Trans. Electron Devices*, vol. 58, no. 5, pp. 1311–1318, May 2011.

[8] H. Kohlstedt, N. A. Pertsev, J. R. Contreras, and R. Waser, "Theoretical current-voltage characteristics of ferroelectric tunnel junctions," *Phys. Rev. B*, vol. 72, p. 125341, Sep. 2005.

[9] M. Y. Zhuravlev, R. F. Sabirianov, S. S. Jaswal, and E. Y. Tsymbal, "Giant electroresistance in ferroelectric tunnel junctions," *Phys. Rev. Lett.*, vol. 94, p. 246802, Jun. 2005.

[10] E. Y. Tsymbal and H. Kohlstedt, "Tunneling across a ferroelectric," *Science*, vol. 313, pp. 181–183, Jul. 2006.

[11] J. P. Velev, C.-G. Duan, K. D. Belashchenko, S. S. Jaswal, and E. Y. Tsymbal, "Effect of ferroelectricity on electron transport in Pt/$BaTiO_3$/Pt tunnel junctions," *Phys. Rev. Lett.*, vol. 98, p. 137201, Mar. 2007.

[12] A. Gruverman *et al.*, "Tunneling electroresistance effect in ferroelectric tunnel junctions at the nanoscale," *Nano Lett.*, vol. 9, pp. 3539–3543, Oct. 2009.

[13] N. A. Zimbovskaya, "Electron transport through asymmetric ferroelectric tunnel junctions: Current-voltage characteristics," *J. Appl. Phys.*, vol. 106, p. 124101, Dec. 2009.

[14] D. Pantel and M. Alexe, "Electroresistance effects in ferroelectric tunnel barriers," *Phys. Rev. B*, vol. 82, p. 134105, Oct. 2010.

[15] S. D. Ha and S. Ramanathan, "Adaptive oxide electronics: A review," *J. Appl. Phys.*, vol. 110, p. 071101, Oct. 2011.

[16] M. Bibes, J. E. Villegas, and A. Barthélémy, "Ultrathin oxide films and interfaces for electronics and spintronics," *Adv. Phys.*, vol. 60, no. 1, pp. 5–84, 2011.

[17] A. Chanthbouala *et al.*, "Solid-state memories based on ferroelectric tunnel junctions," *Nature Nanotechnol.*, vol. 7, pp. 101–104, Feb. 2012.

[18] X. Lu, H. Li, and W. Cao, "Current-voltage characteristics and ON/OFF ratio in ferroelectric tunnel junctions," *J. Appl. Phys.*, vol. 112, p. 054102, Sep. 2012.

[19] D. J. Kim *et al.*, "Retention of resistance states in ferroelectric tunnel memristors," *Appl. Phys. Lett.*, vol. 103, p. 142908, Sep. 2013.

[20] Z. H. Wang *et al.*, "Write operation study of Co/BTO/LSMO ferroelectric tunnel junction," *J. Appl. Phys.*, vol. 114, p. 044108, Jul. 2013.

[21] E. Y. Tsymbal and A. Gruverman, "Ferroelectric tunnel junctions: Beyond the barrier," *Nature Mater.*, vol. 12, pp. 602–604, Jul. 2013.

[22] Z. Wen, C. Li, D. Wu, A. Li, and N. Ming, "Ferroelectric-field-effect-enhanced electroresistance in metal/ferroelectric/semiconductor tunnel junctions," *Nature Mater.*, vol. 12, pp. 617–621, Jul. 2013.

[23] Y. Fujisaki, "Review of emerging new solid-state non-volatile memories," *Jpn. J. Appl. Phys.*, vol. 52, p. 040001, Apr. 2013.

[24] R. Soni *et al.*, "Giant electrode effect on tunnelling electroresistance in ferroelectric tunnel junctions," *Nature Commun.*, vol. 5, Nov. 2014, Art. no. 5414.

[25] Z. Wen, D. Wu, and A. Li, "Memristive behaviors in Pt/$BaTiO_3$/Nb:$SrTiO_3$ ferroelectric tunnel junctions," *Appl. Phys. Lett.*, vol. 105, p. 052910, Aug. 2014.

[26] V. Garcia and M. Bibes, "Ferroelectric tunnel junctions for information storage and processing," *Nature Commun.*, vol. 5, Jul. 2014, Art. no. 4289.

[27] S. Boyn *et al.*, "High-performance ferroelectric memory based on fully patterned tunnel junctions," *Appl. Phys. Lett.*, vol. 104, p. 052909, Feb. 2014.

[28] Z. B. Yan and J.-M. Liu, "Resistance switching memory in perovskite oxides," *Ann. Phys.*, vol. 358, pp. 206–224, Jul. 2015.

[29] S. Boyn *et al.*, "Engineering ferroelectric tunnel junctions through potential profile shaping," *APL Mater.*, vol. 3, p. 061101, Jun. 2015.

[30] S.-I. Kim *et al.*, "Giant electroresistive ferroelectric diode on 2DEG," *Sci. Rep.*, vol. 5, May 2015, Art. no. 10548.

[31] D. Pantel *et al.*, "Tunnel electroresistance in junctions with ultrathin ferroelectric $Pb(Zr_{0.2}Ti_{0.8})O_3$ barriers," *Appl. Phys. Lett.*, vol. 100, p. 232902, Jun. 2012.

[32] N. A. Pertsev, A. G. Zembilgotov, and A. K. Tagantsev, "Effect of mechanical boundary conditions on phase diagrams of epitaxial ferroelectric thin films," *Phys. Rev. Lett.*, vol. 80, pp. 1988–1991, Mar. 1998.

[33] A. M. Bratkovsky and A. P. Levanyuk, "Continuous theory of ferroelectric states in ultrathin films with real electrodes," *J. Comput. Theor. Nanosci.*, vol. 6, pp. 465–489, Mar. 2009.

[34] J. Hlinka and P. Márton, "Phenomenological model of a 90° domain wall in $BaTiO_3$-type ferroelectrics," *Phys. Rev. B*, vol. 74, p. 104104, Sep. 2006.

[35] A. K. Tagantsev, "Landau expansion for ferroelectrics: Which variable to use?" *Ferroelectrics*, vol. 375, no. 1, pp. 19–27, 2008.

[36] S. Prasertchoung, V. Nagarajan, Z. Ma, R. Ramesh, J. S. Cross, and M. Tsukada, "Polarization switching of submicron ferroelectric capacitors using an atomic force microscope," *Appl. Phys. Lett.*, vol. 84, pp. 3130–3132, Apr. 2004.

[37] W. Li and M. Alexe, "Investigation on switching kinetics in epitaxial $Pb(Zr_{0.2}Ti_{0.8})O_3$ ferroelectric thin films: Role of the 90° domain walls," *Appl. Phys. Lett.*, vol. 91, p. 262903, Dec. 2007.

[38] Y. W. Yin *et al.*, "Enhanced tunnelling electroresistance effect due to a ferroelectrically induced phase transition at a magnetic complex oxide interface," *Nature Mater.*, vol. 12, pp. 397–402, May 2013.

[39] A. M. Bratkovsky and A. P. Levanyuk, "Abrupt appearance of the domain pattern and fatigue of thin ferroelectric films," *Phys. Rev. Lett.*, vol. 84, pp. 3177–3180, Apr. 2000.

[40] X. Liu, Y. Wang, J. D. Burton, and E. Y. Tsymbal, "Polarization-controlled Ohmic to Schottky transition at a metal/ferroelectric interface," *Phys. Rev. B*, vol. 88, p. 165139, Oct. 2013.

[41] I. B. Misirlioglu and M. Yildiz, "Carrier accumulation near electrodes in ferroelectric films due to polarization boundary conditions," *J. Appl. Phys.*, vol. 116, p. 024102, Jul. 2014.

Ibrahim Burc Misirlioglu was born in İstanbul. He received his B.Sc. and M.Sc. in Metallurgy (1998) and Materials Science (2001) from İstanbul Technical University. He obtained his Ph.D. degree from University of Connecticut in 2006. He was with Max Planck Institute of Microstructure Physics followed by a researcher position at MIT during 2007–2008. Since 2008, he has been a faculty member in the Faculty of Engineering and Natural Sciences of Sabanci University, İstanbul, Turkey.

Kursat Sendur received his B.S., M.S., and Ph.D. degrees from Middle East Technical University, Ankara, Turkey, Bilkent University, Ankara, Turkey and The Ohio State University, USA respectively. In 2002, he joined Seagate Technologies Research Center, USA. Between 2005 and 2007 he was with Advanced Micosensors, Boston, MA, USA. Since 2007, he has been a faculty member at Sabanci University.